SIMULATION OF HIGH TEMPERATURE, NON-CONGRUENT PHASE TRANSITIONS IN UO_{2+X}

M. J. Welland, B.J. Lewis and W.T. Thompson
Department of Chemistry and Chemical Engineering,
Royal Military College of Canada
PO Box 17000, Station Forces
Kingston, Ontario K7K 3C6

Abstract

A detailed model of UO_{2+x} undergoing non-congruent melting at very high temperature is being developed to help support the design and analysis of experimental work being conducted as part of nuclear safety research. This work includes the simulation of nuclear fuel under upset conditions where centreline melting may occur. The Phase Field model has been implemented for this purpose using recently published material properties and compares well with experimental data. The versatility and robustness of this modelling technique is demonstrated with a simulation of centreline melting in a CANDU fuel element as a consequence of fission heating.

Introduction

Under upset or very high power conditions, it is possible that the temperature at the centreline of a fuel pellet will exceed the local melting point and the fuel will melt. This possibility is enhanced if the fuel element has become defective, in which case the coolant is allowed to contact the UO_2, oxidizing it to UO_{2+x}. Hyperstoichiometric fuel has a reduced thermal conductivity and a lower incipient melting point, thus increasing the temperature at the fuel centreline and the potential for fuel melting.

Recent experiments, typically involving either laser or furnace heating, have been performed to better understand the thermal properties of the sample at high temperature in both the solid and liquid state [1,2]. In order to determine such properties, sophisticated models coupling the heat and mass transport are typically needed [3]. These experiments heat the sample at its surface, however, this is not the case for operational fuel elements which are heated throughout their body by fission. It is therefore useful to generalize these models to include both types of heat sources so that they can be used to deduce material properties from experiments and then employ the same material properties in fuel performance and safety codes.

The thermal and mechanical implications of molten fuel under upset or severe reactor accident conditions have been previously modelled on a large scale for the purpose of reactor safety [4,5,6,7,8]. Detailed simulations have been conducted for defective fuel elements under normal operating conditions [9,10,11], however these simulations do not reach the molten phase. The introduction of a phase transformation adds significant complexity to the fuel behaviour models due to sharply changing material properties. In particular, as a simplification to incorporate such phenomena, the thermal effects of a phase change have been modeled by simply considering rapid changes in the enthalpy or heat capacity over a given temperature interval [12]. A more fundamental treatment, however, is desirable in order to assess such approximate approaches for treating molten fuel behaviour.

The Phase Field model is commonly used in metallurgy to simulate solidification microstructure [13]. It was however found to satisfy the requirements of this work including a fundamental approach to phase change, a robust heat source and the ability to simulate non-congruent phase change. The Phase Field model does not explicitly track the position and rate of propagation of the phase change front but rather can deduce the location of the interface from the solution. The model is derived using the Theory of Irreversible Processes [14,15], and so presents a general and widely applicable framework for the inclusion of many effects.

This work therefore details the development of the Phase Field model towards the simulation of centreline melting in a possibly defected nuclear fuel element. The model is validated first against laser flash experiments that were previously conducted at the Institute for Transuranium elements. The application of the Phase Field model to fuel centerline melting in an operating fuel element is also demonstrated.

Modelling technique

Through experiments in self diffusion, it was discovered that the mobility of oxygen atoms is much larger than that of uranium [16]. Therefore, UO_{2+x} is modelled as an immobile UO_2 lattice with a mobile species of interstitial oxygen atoms denoted by the variable x . The concentration of the mobile interstitial oxygen atoms is equivalent to the deviation of the O/U ratio from 2.

The equations of the Phase Field model can be derived through the Theory of Irreversible Processes in which an extra variable representing the phase change, φ, is added to the temperature T and x. The variable φ is an abstract representation of the extent to which a region of material may be considered to be in one of two phases. It can be interpreted as being proportional to the regularity of atomic spacing [17] and is converted to a volume fraction through a function $p(\varphi)$. In this model, φ varies continuously between *0*, representing the solid phase and *1* representing the liquid, although in general it can represent any two phases. For $\varphi \neq 0,1$, a two phase 'mushy zone' is present in which the local material is a mixture of both phases. This implies that the Phase Field model simulates a diffuse interface, in contrast to the sharp interface used in other models such as the Stefan formulation [18]. This model is very general and can be shown to reduce to the Stefan condition as a special case for the sharp interface limit.

The Theory of Irreversible Processes is founded on the principals of mass conservation, energy conservation and the requirement that local spontaneous processes must increase the amount of entropy in the universe [19]. Due to the small thermal expansion of condensed phases, the volume is assumed to be constant as an approximation. Therefore, in order to conserve mass, the density is treated as a constant. The approximation of constant volume also implies that the thermodynamic functions of internal energy and enthalpy (and therefore the Helmholtz and Gibbs energy) are equal. As derived in the Appendix, the Phase Field model requires the solution of the following set of partial differential equations:

$$\rho Cp\dot{T} = \vec{\nabla}\cdot k\vec{\nabla}T + \dot{Q} - \frac{\partial h}{\partial \varphi}\dot{\varphi} \tag{1}$$

$$\frac{\partial x}{\partial t} = \vec{\nabla}D\left[\nabla x + \frac{\partial\mu/\partial\varphi}{\partial\mu/\partial x}\nabla\varphi\right] \tag{2}$$

$$\frac{\partial \varphi}{\partial t} = -\frac{M_{\varphi}}{T}\left[\frac{\partial g}{\partial \varphi} - \mu\frac{\partial x}{\partial \varphi} - T\varepsilon_{\varphi}^{2}\vec{\nabla}^{2}\varphi\right] + \dot{\varphi}_{n} \tag{3}$$

where ρ is the density of the fuel, Cp is the heat capacity, k is the thermal conductivity, $\dot{Q}$ is volumetric heat generation, D is the chemical diffusion coefficient of interstitial oxygen [16,20], $\dot{\varphi}_n$ is the nucleation rate, M_{φ} is the mobility of φ, μ is the chemical potential of interstitial oxygen, ε_{φ} helps to define the shape of the solid-liquid interface, and g and h are the Gibbs energy and enthalpy densities, respectively. The thermodynamic treatments of UO_{2+x} in the solid and liquid phases are those of a solution of UO_2 and a hypothetical 'UO_3' solute. The treatment faithfully captures the known relationship between oxygen potential, temperature and the O/U ratio in the solid phase [21]. Furthermore, this treatment contributes to a good representation of the entire U-O phase diagram, especially in the area of UO_{2+x} melting [9]. The thermodynamic functions therefore underpin both the equilibrium conditions that exist between phases (as described by the phase diagram) and the kinetics of the melting phenomenon.

Examination of Eq (3) reveals that φ, which describes phase equilibrium, is governed by a free energy minimization equation. In fact, as explained in the Appendix, all three of the presented equations are derived from the principle of entropy maximization.

Material properties between phases are expressed as a linear function of progression of $p(\varphi)$. Using thermal conductivity as an example and denoting the solid and liquid property as subscripts S and L respectively:

$$k = k_S + p(\varphi)\cdot(k_L - k_S) \tag{4}$$

The Phase Field model does not explicitly define the position of the interface, but rather includes it indirectly. This technique allows for complex interface shapes, volumetric heating and undercooling/superheating effects that can pose difficulties in other simulation techniques. Herein lies the power of the Phase Field methodology.

Laser flash experiments

Model implementation

The current model is being validated against laser flash experiments conducted at the Institute for Transuranium Elements [1,22]. These experiments are designed to measure the melting transition in UO_{2+x}, but include data that is useful in the validation of this model. In these experiments, a prepared sample of UO_{2+x} is held in a high pressure helium buffer gas. The purpose of the buffer gas is to suppress vaporization of the sample in which the dominant vapour species is UO_3. As this differs in O/U ratio from that of the condense phase, it will shift the surface O/U ratio and complicate the results. The sample is heated on one side with high intensity laser beam until melting occurs. The intensity of the beam is then reduced to a lower level which helps prevent undercooling effects. The experiment occurs within the time of about 100ms. Due to this short time scale and the pressure of the buffer gas, it is assumed that convective currents in the buffer gas are negligibly small and do not contribute to the heat and mass transfer through the gas. However, as an added precaution, a sapphire window was also placed 1 mm above the sample which would inhibit any gas currents. The surface temperature of the sample is recorded as a function of time by optical pyrometery and is the main result data collected from the experiment.

The laser is assumed to deposit energy uniformly (within the laser spot) in accordance with the expression:

$$q_{laser} = \varepsilon \cdot P_{\max} P_{pulse}(t) \tag{5}$$

where $P_{pulse}(t)$ is the laser power profile, $P_{\max}$ is the maximum power of the laser beam and ε is the emissivity which through Kirchhoff's radiation law [23] is assumed to be equal to the absorbtivity.

Heat is lost from the surface of the sample through conduction into the buffer gas, radiative heat transfer and vaporization:

$$q_{loss} = \frac{k_{He}}{d}\left(T - T_{\infty}\right) + \varepsilon\sigma_{SB}\left(T^4 - T_{\infty}{}^4\right) + \Delta H_{vap} \cdot C_{eff} \cdot \left(\frac{44.3}{\sqrt{M}} \cdot \frac{P_{vap}}{\sqrt{T}}\right) \tag{6}$$

where k_{He} is the thermal conductivity of Helium [24], d is the height of the sapphire window, T_{∞} is the ambient temperature, σ_{SB} is the Stefan Boltzmann's constant, ΔH_{vap} is the molar enthalpy of vaporization, $P_{vap}(T)$ is the vapour pressure [25] and M is the molar mass of the vapour species. The third term in Eq. (6) is the Knudsen effusion formula [26] which is designed for effusion into a vacuum and is used as a simplification of the vapourization process. To correct this for the presence of the buffer gas, this formula includes a constant fraction C_{eff} selected to reproduce the observed temperature profile [12].

Material properties for this simulation are taken from the Fink review [27] unless otherwise referenced.

Results

The results of the simulation of a stoichiometric fuel sample is shown in Figure 1. The discrepancy between the height of the temperature plateaus is due to the choice of the melting temperature. This simulation uses 3120 K as recommended by Fink, whereas a value of 3156 K, at the pressure the experiment was conducted at, is suggested by the experiment. This temperature is a consequence of using the thermodynamic model as previous described. Adjusting this value to match the observations is possible and may constitute part of future development. In this case, however, the difference is small.

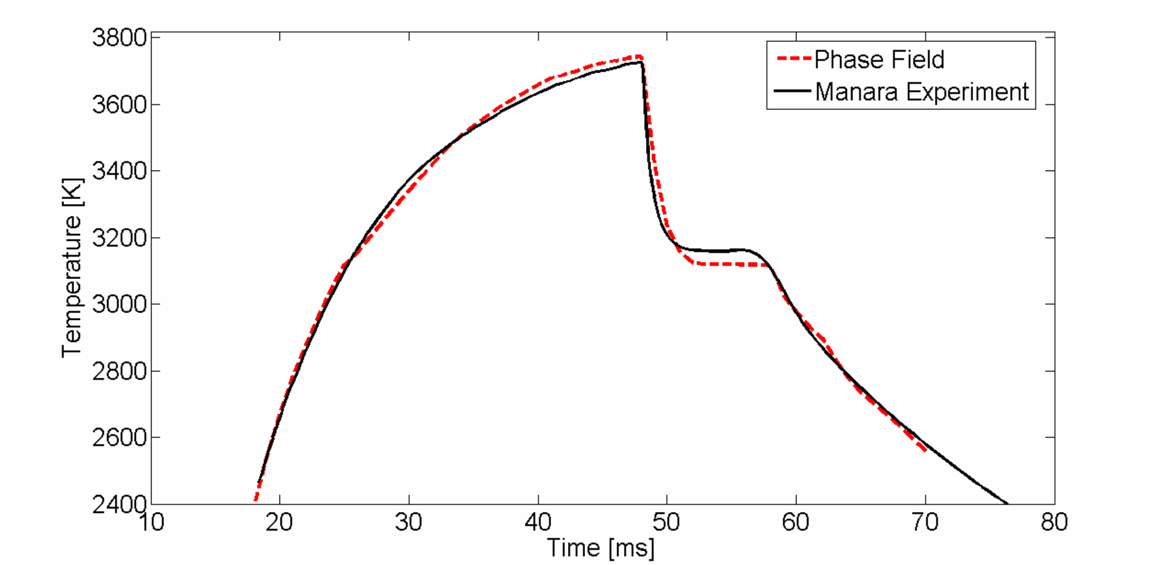

Figure 1: Comparison of experimental data with the phase field model.

In the case of non-stoichiometric fuel, a complex freezing process takes place in which the solute is redistributed as the phase boundary moves. However, this change in local solute concentration changes the melting temperature. Figure 2 shows the calculated temperature and surface O/U ratio in comparison to the observed surface temperature. The calculated temperature and O/U ratio is shown as a function of depth in Figure 3 for the simulation that produced Figure 2 at time 45ms.

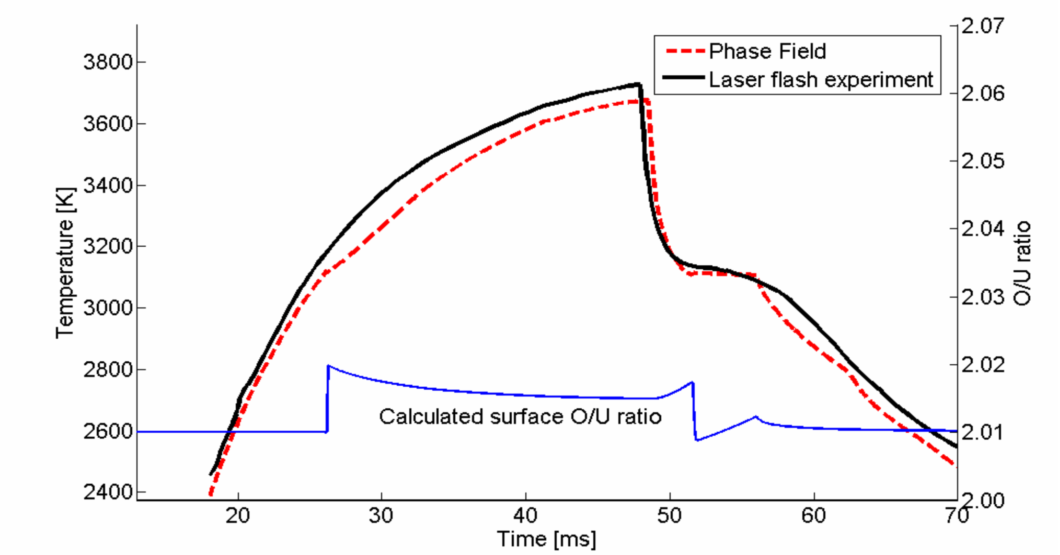

Figure 2: Comparison of the exterimental data with the Phase Field model for UO2.01. The calculated O/U ratio at the surface of the sample is also displayed.

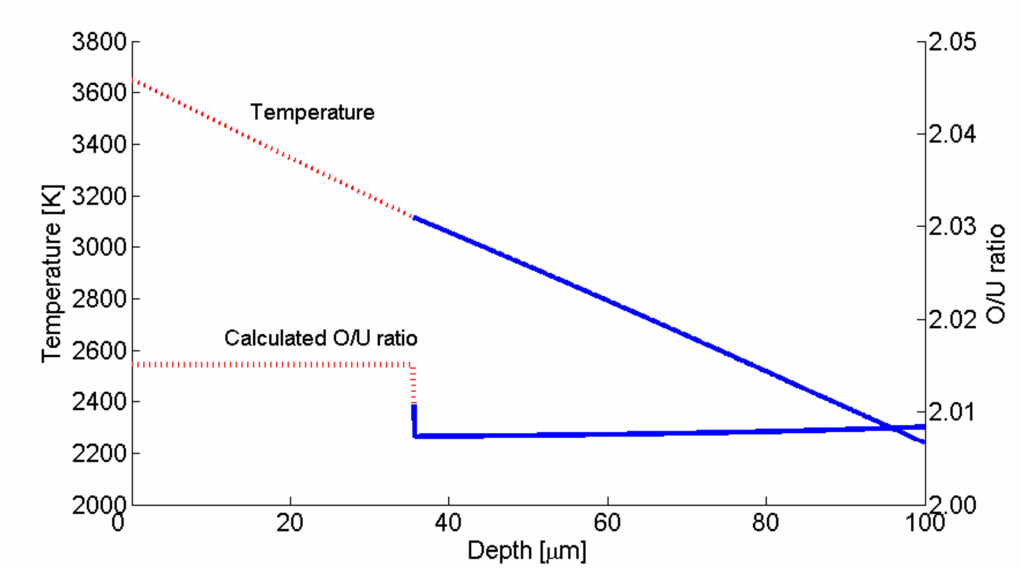

Figure 3: Temperature and O/U profile at 45ms. Solid and broken lines correspond to solid and liquid phases respectively.

Fuel element

Model implementation

Simulation of an operating fuel rod has been performed for an unirradiated, naturally enriched cylindrical fuel pellet. Heat is generated volumetrically through nuclear fission according to:

$$\dot{Q}(r) = \frac{P_{lin}}{\pi a^2}\left[\frac{\kappa a}{2I_1(\kappa a)}\right]I_0(\kappa r) \tag{7}$$

where r is the radius from the centerline, $a = 6.075\ mm$ is the outer pellet radius [9], P_{lin} is the linear power, $\kappa = 0.9cm^{-1}$ is the inverse neutron diffusion length [28] and $I_{0,1}$ are the modified Bessel functions. The temperature at the surface of the pellet is fixed at 700 K and a reflexive condition is set at $r = 0$. Initially, the pellet is a homogenous 700 K and the full linear power is reach instantaneously.

Results

The result of the simulation for a series of linear powers is shown in Figure 4. Centreline melting is predicted at approximately $84\, kW/m$ under these conditions.

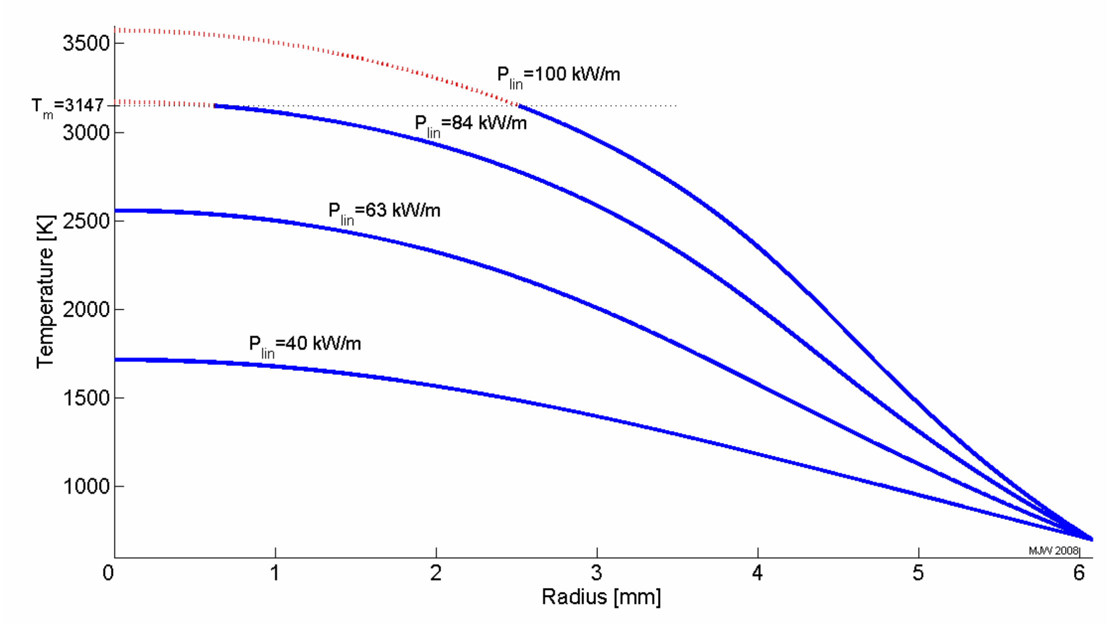

Figure 4: Temperature profiles for fuel elements run at different linear powers, showing centreline melting. Solid and broken lines correspond to solid and liquid phases respectively.

The time dependence of this linear power is shown in Figure 5. For this simulation, no change in the model implementation is required beyond a change in the boundary conditions, the addition of a volumetric heat source and a conversion to cylindrical coordinates. Since the material properties and governing differential equations are unchanged in this analysis, this result demonstrates the versatility of the Phase Field model for use in experimental design and analysis (i.e., to deduce material properties) and for application in safety and fuel performance analysis.

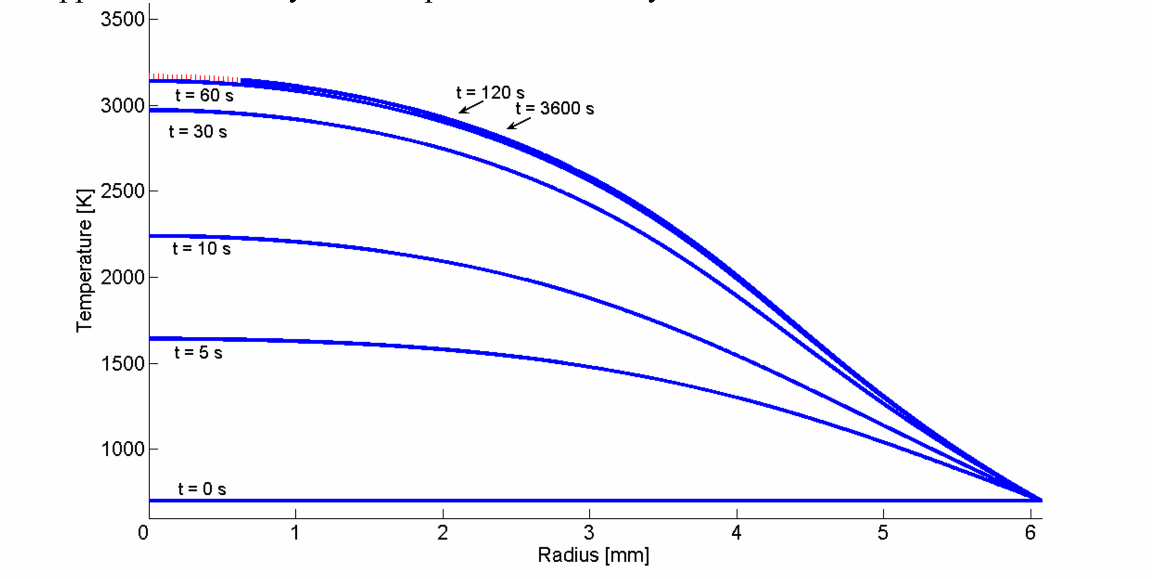

Figure 5: Temperature profiles of a fuel element at *84 kW/m*. Steady state solution with a molten centre is quickly established in about a minute.

Discussion

Examination of the results of the laser flash simulation shows good agreement with experiment. Any disagreement can be partially attributed to the input material properties, some of which are, by necessity, extrapolated well beyond the experimental data while others have a high degree of uncertainty. The effects of the uncertainty in the liquid thermal conductivity, and the choice of density is addressed for the stoichiometric case in [29] and should therefore not lead to a significant difference for the non-stoichiometric situation addressed in this work. The thermal conductivity was shown to primarily affect the depth of the molten pool and thus the length of the solidification plateau. The choice of density was shown to be negligible. The chemical diffusion coefficient used for oxygen diffusion in the solid is recommended up to 1800 K, but is being extrapolated to the melting point. This value mainly influences the distribution of interstitial oxygen which does not substantially affect the results for small hyperstoichiometry. This value will be investigated in future work.

In the simulation of the fuel pellet, as this simulation applies to the stoichiometric case, the main source of uncertainty is the liquid thermal conductivity. The extent of centreline melting depends mostly on the ability to conduct heat away from the centre, through the solid phase. Thus, as the steady state is reached, the thermal conductivity in the liquid has little effect on the extent of the molten zone.

Solving the system of equations for the phase field model requires the definition of a mesh over the region of interest. The resolution of the mesh is a critical factor in determining the computational requirements of the simulation. In order to obtain a good solution, the mesh must be adequately refined in regions where the unknown variables experience large gradients. This poses a challenge in the application of the Phase Field model since φ, by design, varies very sharply between 0 and 1. The sharpness of the interface may be controlled by the user, as described in the appendix. However, a sharper interface is typically desired as it more closely approximates the real situation.

The fact that the position of the interface between phases is not explicitly tracked makes complex interface shapes quite simple to handle. Nucleation and other effects such as constitutional undercooling may also be simulated with this approach.

Conclusions

The Phase Field model is shown to be a versatile and robust modelling technique that is well suited to the simulation of laser flash experiments performed for the purpose of determining material properties and for predicting centreline melting as a result of fission heating in nuclear fuel pellets. Success in including non-stoichiometry in simulating laser flash experiments encourages the continued development of this technique to predicting centreline melting in oxidized fuel elements.

Appendix: Phase Field Derivation

Thermodynamic functions

Thermodynamic functions of internal energy, $u(T,x)$ and entropy, $s(T,x)$ are input parameters for the material system being studied. A binary system of two phases can be written in general as:

$$u(T,x_s,x_L,\varphi) = (1-p(\varphi))u_s(T,x_s) + p(\varphi)u_L(T,x_L) + K(\varphi) \tag{8}$$

where $K(\varphi)$ describes the interfacial energy between two phases. Since the exact nature of φ is unknown, the function $p(\varphi)$ is used to represent the extent to which a volume may be considered as being in either phase. The mole fractions of components in the solid and liquid phases, x_S and x_L, are constrained and related to the overall component mole fraction x:

$$(1-p(\varphi))x_s + p(\varphi)x_L = x \tag{9}$$

If local equilibrium is assumed at the interface, then the partition coefficient k_p can be introduced:

$$x_S = x_L \cdot k_p \tag{10}$$

$$x_L = \frac{x}{k_p \cdot (1-p) + p} \tag{11}$$

Equation (8) may now be written in terms of the overall composition:

$$u(T,x,\varphi) = u_S(T,x) + p(\varphi)[u_L(T,x) - u_S(T,x)] + K(\varphi) \tag{12}$$

The entropy function may similarly be written as:

$$s(T,x,\varphi) = s_S(T,x) + p(\varphi)[s_L(T,x) - s_S(T,x)] \tag{13}$$

where the number of nuclei for one phase in another is assumed to be small enough so that the entropy of mixing two phases is negligible.

The Theory of Irreversible Processes

The local state can be written as $s(u,x,\varphi)$. To determine the total entropy S in a volume V, a general entropy functional is proposed in the form [30, 31]:

$$S = \int_V \left(s(u,x,\varphi) - \frac{\varepsilon_\varphi^2}{2} \left|\vec{\nabla}\varphi\right|^2 \right) \mathrm{dV} \tag{14}$$

where $s(u,x,\varphi)$ is the local entropy density given as a function of the concentration of a solute x, the phase field variable φ , and the internal energy density $u(T,x,\varphi)$, which is a function of the temperature T, x and φ. The constant ε_φ multiplies the squared magnitude of the gradient in φ to account for the energy effect of a gradient in φ. Using dot notation to indicate time derivatives, the rate of change of the entropy may be derived:

$$\frac{\mathrm{d}S}{\mathrm{d}t} = \int_V \left(\left.\frac{\partial s}{\partial u}\right|_{c,\varphi} \dot{u} + \left.\frac{\partial s}{\partial x}\right|_{u,\varphi} \dot{x} + \left.\frac{\partial s}{\partial \varphi}\right|_{u,x} \dot{\varphi} - \varepsilon_\varphi^2 \vec{\nabla}\varphi \vec{\nabla}\dot{\varphi} \right) \mathrm{d}V \tag{15}$$

The subscripted variables beside the derivatives are inserted to specify the variables being held constant and to emphasize that the internal energy is also a function of T, x and φ. In this model, the density, and therefore concentration of U atoms, is held constant. Neglecting nuclear reactions, the laws of conservation of energy and mass are:

$$\dot{u} + \vec{\nabla}\cdot\vec{J}_u = \dot{Q} \tag{16}$$

$$\dot{x} + \vec{\nabla}\cdot\vec{J}_x = 0 \tag{17}$$

where $\vec{J}_u$ is the flux[1] of internal energy (heat flux) and $\vec{J}_x$ is the flux of interstitial oxygen. This equation can be substituted into Eq. (15) and rearranged through Green's Theorem and the Divergence Theorem to yield:

$$\begin{aligned}\underbrace{\frac{\mathrm{d}S}{\mathrm{d}t}}_{\textit{Entropy change}} &= \underbrace{\int_V \left(\vec{\nabla}\left.\frac{\partial s}{\partial u}\right|_{x,\varphi}\cdot\vec{J}_u + \vec{\nabla}\left.\frac{\partial s}{\partial x}\right|_{u,\varphi}\cdot\vec{J}_x + \left[\left.\frac{\partial s}{\partial \varphi}\right|_{u,x} + \varepsilon_{\varphi}^{2}\vec{\nabla}^{2}\varphi\right]\dot{\varphi}\right)\mathrm{dV}}_{\textit{Entropy produced by irreversible processes}} \\ &- \underbrace{\int\left(\left.\frac{\partial s}{\partial u}\right|_{x,\varphi}\cdot\vec{J}_u + \left.\frac{\partial s}{\partial x}\right|_{u,\varphi}\cdot\vec{J}_x + \varepsilon_{\varphi}^{2}\dot{\varphi}\vec{\nabla}\varphi\right)\cdot\hat{n}\,\mathrm{d}A}_{\textit{Entropy flux across boundary}} + \underbrace{\int\left(\frac{\partial s}{\partial u}\cdot\dot{Q}\right)\mathrm{dV}}_{\textit{Volumetric generation}}\end{aligned} \tag{18}$$

where A is the boundary of V and the last term accounts for entropy introduced into the system that is not a result of a flux across the boundary or an internal irreversible process.

As the entropy produced in a system is always positive for a real system and since the first term on the right hand side of Eq. (18) is valid for an arbitrary volume then:

$$\vec{\nabla}\left.\frac{\partial s}{\partial u}\right|_{x,\varphi}\cdot\vec{J}_u + \vec{\nabla}\left.\frac{\partial s}{\partial x}\right|_{u,\varphi}\cdot\vec{J}_x + \left[\left.\frac{\partial s}{\partial \varphi}\right|_{u,x} + \varepsilon_{\varphi}^{2}\vec{\nabla}^{2}\varphi\right]\dot{\varphi} \geq 0 \tag{19}$$

This inequality may be ensured if the fluxes are assumed to be proportional to their conjugate thermodynamic driving forces. Defining the proportionality factors to be the mobility of the state property:

$$\vec{J}_u = M_u\vec{\nabla}\left.\frac{\partial s}{\partial u}\right|_{x,\varphi} \tag{20}$$

$$\vec{J}_x = M_x\vec{\nabla}\left.\frac{\partial s}{\partial x}\right|_{u,\varphi} \tag{21}$$

$$\dot{\varphi} = M_{\varphi}\left(\left.\frac{\partial s}{\partial \varphi}\right|_{u,x} + \varepsilon_{\varphi}^{2}\vec{\nabla}^{2}\varphi\right) \tag{22}$$

Equation (19) may be assured by stating that the proportionality factors, the mobilities $M_u, M_x, M_{\varphi} > 0$. The definition of thermodynamic temperature is now employed:

$$\left.\frac{\partial s}{\partial u}\right|_{x,\varphi} = \frac{1}{T} \tag{23}$$

Commonly, the function $s(u(T,x,\varphi),x,\varphi)$ is not available. Thus it is convenient to express derivatives of this function in terms of functions of the independent variables:

---

[1] The notion of a flux in this application is typical of applications in heat and mass transfer and is equivilant to the concept of a current in neutron physics.

$s(T,x,\varphi)$ and $u(T,x,\varphi)$. Through the use of eq. (23) and the total derivative, it can be shown that:

$$\begin{aligned}\frac{\partial s(T,x,\varphi)}{\partial x} &= \left.\frac{\partial s(u,x,\varphi)}{\partial x}\right|_{u,\varphi} + \left.\frac{\partial s(u,x,\varphi)}{\partial u}\right|_{x,\varphi}\frac{\partial u(T,x,\varphi)}{\partial x} \\ \left.\frac{\partial s(u,x,\varphi)}{\partial x}\right|_{u,\varphi} &= -\frac{1}{T}\frac{\partial g(T,x,\varphi)}{\partial x}\end{aligned} \qquad (24)$$

in which the approximation of a constant volume is again invoked so as to use the Gibbs energy in place of Helmholtz energy, $g \cong u - Ts$.

Similarly:

$$\begin{aligned}\frac{\partial s(T,x,\varphi)}{\partial \varphi} &= \frac{1}{T}\frac{\partial u(T,x,\varphi)}{\partial \varphi} + \left.\frac{\partial s(u,x,\varphi)}{\partial x}\right|_{u,x}\frac{\partial x}{\partial \varphi} + \left.\frac{\partial s(u,x,\varphi)}{\partial \varphi}\right|_{u,x} \\ \left.\frac{\partial s(u,x,\varphi)}{\partial \varphi}\right|_{u,x} &= -\frac{1}{T}\left[\frac{\partial g(T,x,\varphi)}{\partial \varphi} - \frac{\partial g(T,x,\varphi)}{\partial x}\frac{\partial x}{\partial \varphi}\right]\end{aligned} \qquad (25)$$

Equations (20) and (21)and may now be rewritten in terms of the Gibbs energy using (23), (24) and (25). Using the definition of the chemical potential, $\mu = \partial g/\partial x$:

$$\vec{J}_u = -\frac{M_u}{T^2}\nabla T \qquad (26)$$

$$\vec{J}_x = -\frac{M_x}{T}\nabla \mu \qquad (27)$$

$$\dot{\varphi} = -\frac{M_\varphi}{T}\left[\frac{\partial g(T,x,\varphi)}{\partial \varphi} - \mu\frac{\partial x}{\partial \varphi} - T\varepsilon_\varphi^2\vec{\nabla}^2\varphi\right] \qquad (28)$$

Through comparison with Fourier heat transport, $\vec{J}_u = -k\nabla T$, the value of M_u may be determined from Eq. (26)

$$k = -\frac{M_u}{T^2} \qquad (29)$$

The gradient in Eq. (27) can be expanded in terms of gradient of the state variables:

$$\vec{J}_x = -\frac{M_x}{T}\left[T\frac{\partial}{\partial T}\left(\frac{\mu}{T}\right)\nabla T + \frac{\partial \mu}{\partial x}\nabla x + \frac{\partial \mu}{\partial \varphi}\nabla \varphi\right] \qquad (30)$$

If isothermal diffusion in a single phase is considered, Fickian diffusion is recovered:

$$\vec{J}_x = -\frac{M_x}{T}\frac{\partial \mu}{\partial x}\nabla x = -D\nabla x \qquad (31)$$

where D is the chemical diffusion coefficient.

$$\frac{M_x}{T} = \frac{D}{\partial \mu/\partial x} \qquad (32)$$

The approximation of negligible expansion of the condensed phases implies that the internal energy may be replaced by the enthalpy and so:

$$\begin{aligned}\frac{\partial h}{\partial t} &\cong \frac{\partial u}{\partial t} \\ &= \rho C p \dot{T} + \frac{\partial h}{\partial x}\dot{x} + \frac{\partial h}{\partial \varphi}\dot{\varphi}\end{aligned} \tag{33}$$

where the definition $\partial h / \partial t = \rho C p$ has been used.

The effects of the first term in (32), and the second term in (35) have been assumed to be negligible in the current model due to the small deviation from stoichiometry (*x = 0.01*). The effects of these terms will be further explored and implemented for higher degrees of oxidation. Therefore, the flux equations (26) and (30) and the conservation equations: (16) and (17) may be combined and summarized to yield a set of differential equations that constitutes the Phase Field model:

$$\rho C p \dot{T} = -\frac{\partial h}{\partial \varphi}\dot{\varphi} + \vec{\nabla} \cdot k \vec{\nabla} T + \dot{Q} \tag{34}$$

$$\dot{x} = \vec{\nabla} D \left[\nabla x + \frac{\partial \mu / \partial \varphi}{\partial \mu / \partial x} \nabla \varphi \right] \tag{35}$$

and

$$\dot{\varphi} = -\frac{M_\varphi}{T}\left[\frac{\partial g(T, x, \varphi)}{\partial \varphi} - \mu \frac{\partial x}{\partial \varphi} - T \varepsilon_\varphi^2 \vec{\nabla}^2 \varphi \right] \tag{36}$$

Phase Field parameters

Within the confines of certain constraints [32], the actual form of these equations is arbitrary insofar as the choice does not affect the sharp interface limit. For this implementation, a common choice is employed [14]:

$$p(\varphi) = \varphi^3 [6\varphi^2 - 15\varphi + 10] \tag{37}$$

$$K_u(\varphi) = W \varphi^2 [1 - \varphi]^2 \tag{38}$$

where W can be related to excess energy molecules of interfacial material.

Through considerations of an isothermal, steady state solution to Eq. (3), the constants W and ε_φ can be shown to relate to the excess interfacial energy σ and a user defined measure of the interface width δ by the equations [14,33]:

$$W = 6\sigma / \delta \tag{39}$$

$$\varepsilon_\varphi^2 = 12\sigma\delta / T_m \tag{40}$$

The mobility of φ, M_φ corresponding to the rate of phase growth is related to the interface kinetics. Since solidification kinetics is not in the scope of this work, this value was selected to ensure that the interface position propagated with the local melting temperature.

Nucleation is introduced *ad hoc* into Eq. (36) through $\dot{\varphi}_n$ in a simple form derived from basic nucleation theory [34]:

$$\dot{\varphi}_n = \exp\left(-\frac{\Delta G_n^o}{k_B T}\right)\cdot\begin{cases} I_S^o(1-\varphi) & \mathit{if}\ \Delta G < 0 \\ -I_L^o\varphi & \mathit{if}\ \Delta G > 0 \end{cases} \tag{41}$$

where ΔG_n^o is the critical energy for a nucleus, k_B is Boltzmann's constant, ΔG is the change in free energy between phases, and the constants $I_{S,L}^o$ are related to nucleation kinetics. This equation is essentially an Arrhenius equation with and activation energy ΔG_n^o which depends on the surface energy σ, and the heterogeneous nucleation factor, f_θ:

$$\Delta G_n^o = \frac{16\pi}{3}\left(\frac{\sigma^3}{(\Delta G/\rho)^2}\right)f_\theta \tag{42}$$

References

[1] D. Manara, C. Ronchi, M. Sheindlin, M. Lewis and M. Brykin, J. Nucl. Mater. 342 (2005) 148.
[2] R. E. Latta and R. E. Fryxell, J. Nucl. Mater., 35 (1970) 195.
[3] V. Atrazhev and M. Brykin, Numerical simulation of melting and solidification of binary mixtures in laser heating pulses (non-congruent phase transition solid-liquid), Study Contract N. 17644-2001-03F1SC KAR RU Final Report (ITU).
[4] C. M. Allison, G. A. Berna, L. J. Siefken, Draft preliminary report for comment: SCDAP/MOD1 theory and models, (Idaho National Engineering Laboratory informal report, 1985).
[5] W.J. Camp, M.F. Young, J.L. Tomkins, J.E. Kelly, P.J. Maudlin and R,J. Henninger, "MELPROG-PWR/MODO: A Mechanistic Code for Analysis of Reactor Core Melt Progression and Vessel Attack Under Severe Accident Conditions, NUREG/CR-4909 SAND85-0237 R3, Sandia National Laboratories, April 1987.
[6] H.E. Sills, "ELOCA Fuel Element Behaviour During High-Temperature Transients, Atomic Energy of Canada Limited report, AECL-6357, March 1979.
[7] M.S. Veshchunov, R. Dubourg, V.D. Ozrin, V.E. Shestak, V.I. Tarasov, R. Dubourg and G. Nicaise, "Development of mechanistic code MFPR for modelling fission product release from irradiated UO2 fuel," Nucl. Eng. Des. 236 (2006) 179-200.
[8] M.S. Veshchunov, V.D. Ozrin, V.E. Shestak and V.I. Tarasov, "Mechanistic modelling of urania fuel evolution and fission product migration during irradiation and heating," J. Nucl. Mater. doi:10/1016/jnucmat 2007.01.081, January 2007.
[9] J.D. Higgs, B.J. Lewis, W.T. Thompson and Z. He, J. Nucl. Mater. 366 (2007) 99.
[10] B. J. Lewis, W. T. Thompson, F. Akbari, D. M. Thompson, C. Thurgood and J. Higgs, J. Nucl. Mater. 328 (2004) 180.
[11] J.C. Ramirez, M. Stan and P. Cristea, "Simulations of heat and oxygen diffusion in UO_2 nuclear fuel rods," J. Nucl. Mater. 359 (2006) 174-184.
[12] M. Sheindlin, D. Staicu, C. Ronchi, L. Game-Arnaud, B. Remyand, A. DeGiovanni, J. Appl. Phys. 101 (2007).
[13] J. C. Ramirez, C. Beckermann, A. Karma and H.-J. Diepers, Phys. Rev. E 69 (2004).
[14] W. J. Boettinger, J. A. Warren, C. Beckermann and A. Karma, Annu. Rev. Mater. Res. 32 (2002) 163.
[15] Z. Bi, R. F. Sekerka, Physica A, 261 (1998) 95.
[16] J. A. Meachen, Nucl. Energy, 28 (1989) 221
[17] U. Hecht, L. Gránásy, T. Pusztai, et al., Materials Science and Engineering R 46 (2004) 1.
[18] M. J. Welland, B. J. Lewis and W. T. Thompson, in: Proceedings of the 30th CNS/CSA student conference, CNS-SNC 2006.
[19] S. R. deGroot and P. Mazur, Non-equilibrium thermodynamics, General Publishing Company, Ltd., Toronto, ON 1984.

[20] B. J. Lewis et al. J. Nucl. Mater. 227 (1995) 83.
[21] T. B. Lindemer and T. M. Besmann, J. Nucl. Mater. 130 (1985) 473.
[22] D. Manara, Melting transition measurements in Uranium Dioxide, PhD thesis, University of Warwick, (2004).
[23] J. R Welty, C. E. Wicks, R. E. Wilson, Fundamentals of momentum, heat and mass transfer, 3rd ed, John Wiley & Sons, Inc., New York 1984.
[24] N. B. Vargaftik and Y. D. Vasilvskaya, J. Eng. Phys., 42 (1982) 296.
[25] M. Tetenbaum and P. D. Hunt, J. Nucl. Mater. 34 (1970) 86.
[26] B. J. Lewis, B. J. Corse, W. T. Thompson, M. H. Kaye, F. C. Iglesias, P. Elder, R. Dickson, Z. Liu, J. Nucl. Mater. 252 (1998) 235.
[27] J. K. Fink, J. Nucl. Mater. 279 (2000) 1.
[28] D. Morgan, A thermomechanical model of CANDU fuel, MASc, Royal Military College of Canada (2007)
[29] M. J. Welland, B. J. Lewis, W. T. Thompson, *J. Nucl. Mater.* In Press
[30] O. Penrose and P. C. Fife, Physica D 43 (1990) 44.
[31] R. F. Sekerka, J. Cryst. Growth, 264 (2004) 530.
[32] S. L. Wang, R. F. Sekerka, A. A. Wheeler, B. T. Murray, S. R. Coriell, R. J. Braun, and G. B. McFadden, Thermodynamically-consistent Phase Field models for solidification, *Physica D*, 69 p189 (1993).
[33] M. J. Welland, W. T. Thompson, B. J. Lewis, Computer simulation of non-congruent melting of non-stoichiometric uranium dioxide fuel, In: Proceedings of the 2007 International LWR Fuel Performance Meeting, San Francisco, California (2007).
[34] K. Fisher, “Fundamentals of Solidification”, 4th Ed, Trans Tech Publishing Ltd. Uetikon-Zuerich, Switzerland (1998)